Tribology International 189 (2023) 108991

Contents lists available at ScienceDirect

Tribology International

journal homepage: www.elsevier.com/locate/triboint

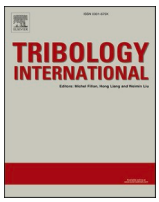

Theoretical analysis and experimental tests of tilting pad journal bearings with shoes made of polymer material and low-boiling liquid lubrication

Grzegorz Żywica [a,*], Artur Olszewski [b], Paweł Bagiński [a], Artur Andrearczyk [a], Tomasz Żochowski [b], Piotr Klonowicz [a]

[a] Institute of Fluid–Flow Machinery, Polish Academy of Sciences, Fiszera 14, 80–231 Gdańsk, Poland
[b] Gdańsk University of Technology, Faculty of Mechanical Engineering and Ship Technology, Narutowicza 11–12, 80–233 Gdańsk, Poland

ARTICLE INFO

Keywords:
High-speed bearing
Tilting pad bearing
Polymeric bearings
Microturbine
Low-boiling liquid

ABSTRACT

Selecting the appropriate bearing system for the rotor requires a good knowledge of the available solutions and the operating conditions of the machine. For newly designed machinery operating in adverse conditions, selecting bearings that ensure correct and long-lasting operation can be extremely challenging. Difficulties increase when the machine's operating parameters are beyond the technical capabilities of available technical solutions. This article presents the course of the design process and results of numerical and experimental research of a prototype microturbine that uses an innovative rotor-bearing system. Due to the adverse operating conditions, new tilting pad journal bearings were designed, in which the sliding surfaces of the tilting pads were made of polymeric material and a low-viscosity medium in liquid form was used as the lubricating medium. The basic bearing parameters were selected and pre-checked by numerical calculations. The oil-free turbomachinery design thus developed was subjected to experimental testing under near-real conditions. The results of these tests confirmed that the developed bearings performed very well, ensuring stable operation of the high-speed rotor of the microturbine over a wide speed range. Despite the unfavourable lubrication conditions, no signs of bearing wear were observed. The results obtained indicate a new, promising direction for the development of bearing systems for turbomachinery, in which, with a suitable design of the bearings, a low-boiling working medium in liquid form can be used as a lubricating medium.

1. Introduction

The development of modern turbomachinery is associated with overcoming many technical, environmental and economic barriers. This requires considering often conflicting requirements and finding the optimal solution for specific operating conditions. Due to the fact that legal and ecological aspects have been given a lot of attention in recent years, not every innovative design, even an excellent one from a technical point of view, is developed and finally reaches the market as a finished product. This applies to a wide range of turbomachinery such as steam and gas turbines or compressors, which are used in many areas of the economy.

Due to environmental concerns and the high prices of energy-producing raw materials, much attention has been paid to small-scale energy generation and energy recovery from various production processes in recent years. In this regard, microturbines operating on the basis of the organic Rankine cycle (ORC) are becoming more widely used. Such cycles use various types of low-boiling mediums, allowing the system to operate in a much lower temperature range than is the case with classical cycles using water as the working medium [1,2]. ORC cogeneration systems with vapour microturbines allow the simultaneous generation of heat and electricity on a small scale or the use of low- and medium-temperature waste heat for energy needs [3,4]. By using innovative design solutions for the microturbines used in ORC systems, these machines can operate within a wide range of operating parameters and achieve high efficiency in converting thermal energy into electricity [5,6]. Modern ORC microturbines, for example, use direct (gearless) drives for their high-speed generators, blade systems with a supersonic flow, and oil-free hermetically-sealed casings [7,8]. Compared to conventional high-capacity energy turbines, microturbines are characterised by significantly smaller dimensions, higher rotational speeds and the ability for long-term operation beyond the nominal operating point (across a wide range of rotational speeds and loads). Such solutions have the advantage of being smaller in size and weight. This is especially

* Corresponding author.
E-mail address: gzywica@imp.gda.pl (G. Żywica).

https://doi.org/10.1016/j.triboint.2023.108991
Received 30 July 2023; Received in revised form 15 September 2023; Accepted 27 September 2023
Available online 29 September 2023

important when deploying low-power units in non-industrial settings, given the limited space available for such installations [9].

Growing environmental awareness and increasingly stringent environmental standards are forcing researchers to seek alternative bearing lubrication methods, which until now have relied on the use of traditional lubricants such as oils, which are potentially harmful to the environment. At present, there is a growing use of newly proposed bearing lubrication methods. Gas bearings are often used in high-speed machines [10]. Many examples of the use of magnetic bearings are also known [8,11]. Also, new materials are providing increasing opportunities to eliminate or replace traditional lubricants. Examples include bearings that use ceramic components or metal-ceramic composites [12]. However, these solutions have certain limitations. For example, gas bearings have low load capacities, and ceramic bearings have a limited life, especially at high rotational speeds [13]. Magnetic bearings have many advantages, but they are still much more expensive than classic rolling and plain bearings [14]. In response to these challenges, there is a growing interest in plain bearings that can be lubricated with unconventional lubricants, such as low-boiling fluids used as working mediums in ORC systems [15]. In such a system, the bearing lubricant can be supplied directly from the machine's working cycle, either in the form of a gas or a liquid. When it comes to microturbines used in ORC systems, this bearing lubrication solution enables the construction of oil-free microturbines [16]. Choosing the right bearing design and the right lubrication method is one of the biggest challenges in designing new turbomachinery. In addition to fulfilling the basic function of transferring the load from the rotating shaft to the bearing supports, bearings must also provide adequate precision of movement and acceptable dynamic properties. High durability and reliability are also desirable. In addition, the low friction losses of the bearings improve the overall efficiency of the machine. When it comes to ORC systems, the high flow efficiency of a microturbine can only be achieved at high rotational speeds [5,17], which is associated with flow parameters. Therefore, the bearing methods commonly used for low-speed machines do not work well for ORC microturbines.

Based on the available technologies and their own experience with high-speed turbomachinery bearings, the authors of this article turned their attention to tilting pad bearings (TPBs) when designing a new ORC turbogenerator. Tilting pad journal bearings are characterised by very good dynamic properties, providing the possibility of stable rotor operation at high rotational speeds [18]. Thanks to their favourable properties, these types of bearings can also be used to support rotors that operate in a vertical position [19,20]. Their unique design allows for self-adjustment, which translates into stable operation under various load conditions. However, the disadvantage of these bearings can be that they are more sensitive to changes in the viscosity of the lubricant, for example at lower temperatures. The experimental work of other researchers has shown that an increase in oil temperature, leading to a reduction in viscosity, can result in an increase in vibration amplitude, which is particularly noticeable at high rotational speeds [21]. These studies have provided a better understanding of the dynamic characteristics of a turboexpander rotor supported by TPBs. On the other hand, the authors of the work [22], investigating the correlation between the increase in rotational speed, the logarithmic decrement of damping and the temperature of the lubricant at the inlet, demonstrated that the stability of a rotor supported by TPBs can be improved within a certain range by a controlled increase in the inlet oil temperature. Lubricant temperature also has a significant impact on power losses. By changing the configuration of the TPB, the dynamic stability can be significantly improved and the friction losses of the TPBs can be reduced [22,23]. Examples of analyses covering the identification of the dynamic coefficients of TPB are presented in works [24] and [25]. In the case of such bearings, it should be noted that the friction between the tilting pad and the sleeve, which occurs at the pad support point, also affects their characteristics [26]. The deformations of the pads are also not insignificant. The authors of the work [27] proposed analysis methods for TPB that enable the prediction of individual pad deformations. An important aspect is the accuracy of the prediction of the dynamic coefficients of TPB. The studies discussed in the works [18,28] include the analysis and experimental determination of the stiffness coefficients of such bearings. Other researchers [29,30] have considered factors such as surface porosity and mixed lubrication in their studies of TPBs. When analysing TPBs, some researchers also make attempts to consider turbulence and thermal effects, which can have an impact on the load capacity of the lubricating film and the dynamics of the rotor–bearings system [31]. Accurate models of TPBs, which take into account the specific features of these types of bearings, enable more accurate predictions of their characteristics under various operating conditions.

This article proposes the concept of TPB lubrication using a low-boiling medium in liquid form. In order to increase the durability and reliability of a bearing lubricated with a low-viscosity liquid, it was proposed to use tilting pads with sliding surfaces made of a selected polymer. Such a combination of an unconventional lubricant with an atypical material from which the tilting pads are made is a new solution that has not been presented in the literature to date. The few previously published papers presented studies of plain bearings with components made of polymeric materials [32–35], but none of these bearings used a low-boiling medium in liquid form as a lubricant. The following sections of the article discuss the most important stages of work on new bearings, including the development of their design and its optimisation, the fabrication work on a prototype bearing and the experimental testing of the bearings in a prototype microturbine. The modelling method used and the analyses of the TPB proved effective and enabled the correct design of an atypical bearing that successfully passed the first tests under laboratory conditions.

2. Bearing system concept

2.1. Analysis of bearings lubricated with a low-boiling medium

For the correct operation of a turbomachine, it is necessary to select suitable bearings that are capable of effectively transmitting the different types of loads acting on the rotor over the entire range of rotational speed. When designing a new machine with an innovative bearing system, a very thorough bearing analysis is required, including the selection of selected bearing parameters and the verification of their basic characteristics through calculation methods.

Due to the requirement for high durability and reliability, as well as low vibration and noise levels, the decision was made to use hydrodynamic bearings to support the rotor in the designed microturbine (Fig. 1). To reduce the possibility of mixing the low-boiling medium with oil and simplify the microturbine design, the decision was made to lubricate the bearings with a working medium sourced from the ORC system cycle. In order to ensure adequate load capacity of the bearings, it was assumed that the bearings would be lubricated with a low-boiling medium in liquid form, rather than in a gaseous form as seen in previously developed lower-power energy microturbines [7,36]. Such a solution makes it possible to dispense with an additional oil lubrication system for bearings and a heavy-duty sealing system, which increases the reliability of the entire machine. The use of classical oil bearings requires the use of special seals that separate the oil cycle from the working medium cycle and the use of an oil system with components such as a pump, filters, a tank and control valves.

The bearings were lubricated with a low-boiling fluid known as "MM" (hexamethyldisiloxane), which was also used as the working medium for the microturbine. This required an individual approach during the bearing design process and careful selection of its geometry. The design calculations assumed that the low-boiling medium has a temperature of 60 °C at the inlet to the bearings. At this temperature, this medium has a density of 726.86 kg/m^3 and a dynamic viscosity of 0.000335 N·s/m^2. The viscosity of the liquid used is therefore approximately 50 times less than that of typical lubricants used in plain bearings and even lower than

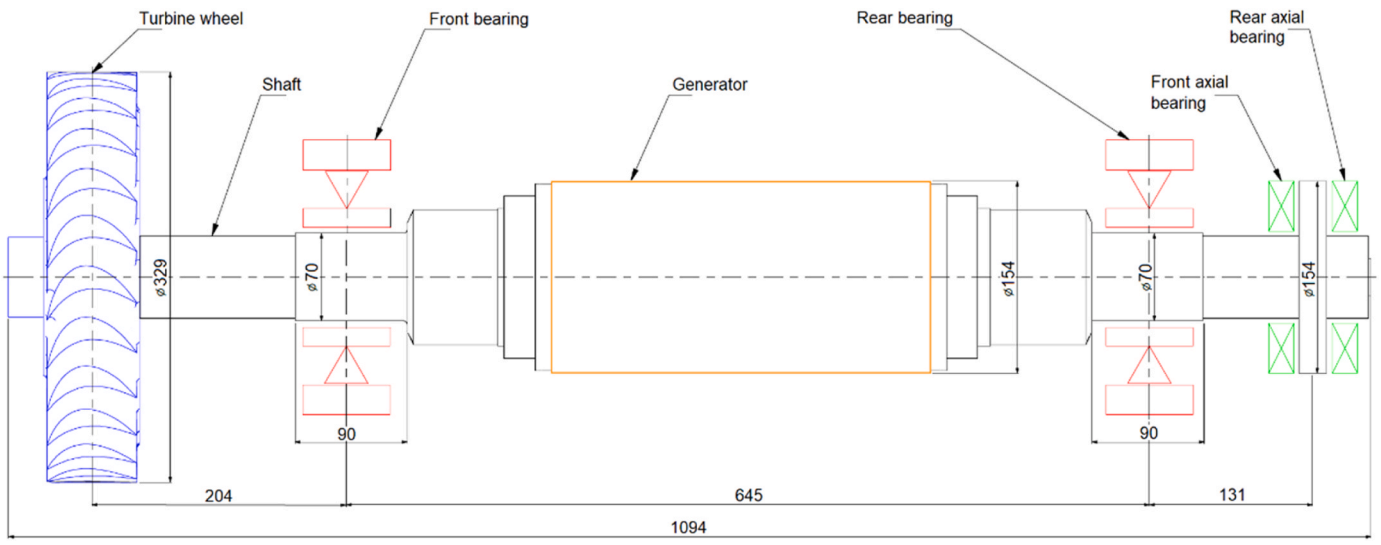

Fig. 1. Schematic diagram and basic dimensions of the 300 kW ORC microturbine rotor.

that of water. Therefore, in the designed bearing, the decision was made to use tilting segments made of special plastic, the selection of which is discussed in the further part of the article.

Calculations performed at the design stage included determining the characteristics of several geometric variants of the tilting pad bearing with a nominal diameter of 70 mm. This diameter did not change during the calculations, as it was consistent with the diameter of the journals of the microturbine shaft. Other parameters were changed to select the best design variant. The main criteria in choosing the bearing geometry were to achieve the greatest possible thickness of the lubricating film and ensure stable operation of the bearing across the entire range of operating speeds. The analyses performed included the arrangement of the tilting pads (in accordance with Fig. 2), the modification of the bearing width and the selection of the radial clearance and preload. The bearing length was changed within a range of 42–50 mm. The radial clearance analysed encompassed a range of 0.05–0.09 mm and the preload value ranged from 0 to 0.5. Finally, after conducting several series of calculations, the decision was made to select the bearing with tilting pads arranged according to Fig. 2a, which had a width of 45.7 mm and a radial clearance of 0.0525 mm. Each pad was supported at half-length, and the output value of the preload was 0 (the pads were not shifted towards the centre of the bearing). It is worth adding that, despite the lack of preload in the output variant of the bearing, its design allows the introduction of preload by adjusting the support height of the pads. The ORC microturbine for which the bearing in question is designed will use two identical tilting pad carrier bearings. Both bearings will operate under similar conditions, so making changes to their design would not be justified. Due to the very extensive set of calculation results obtained during the bearing analysis and design phase, only the most important characteristics obtained for the finally selected bearing variant are presented in the further part of this section.

The calculations were performed using specialised software called Madyn 2000, which is dedicated to the analysis of bearings and complex rotating systems [37]. Hydrodynamic bearings with tilting pads of any geometry can be analysed in this program [38]. Before starting the calculations, it was necessary to supplement the library of this program with the properties of the lubricating liquid used. The density and viscosity of the lubricant at a temperature of 60 °C were assumed in accordance with the previously mentioned values. As the lubricant used has a low viscosity, it is anticipated that there will be a slight increase in temperature. Therefore, a constant adiabatic bearing model ~~of a bearing~~ was used in the calculations. In this model, the fluid film temperature remains constant and is utilised as the mean temperature. This bearing analysis takes into account turbulence and the Reynolds number and therefore it employs another dependency in addition to the Sommerfeld number [38]. The Madyn 2000 software also uses a more advanced thermal model of the bearing (a variable adiabatic model), in which parameters such as the density and viscosity of the lubricant can vary

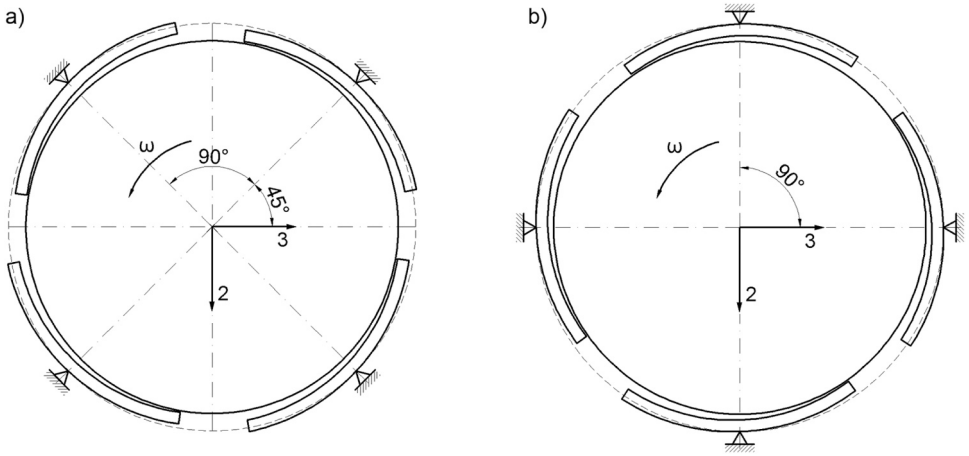

Fig. 2. Two alternative solutions for a four-segment bearing with tilting pads (a – journal supported by two pads, b – journal supported by one pad).

with temperature. However, none of these models considers changes in the rheological properties of the lubricant. The full geometry of the bearing was taken into account, including the self-adjustment of the segments. The static load of the journal bearings, which was determined on the basis of the reactions at the rotor support points, was 482 N for the bearing mounted on the side of the rotor disc (front bearing) and 358 N for the bearing mounted on the side of the thrust plate (rear bearing). The given bearing designations are shown in Fig. 1. The calculations were performed in a speed range of 2,000 rpm to 30,000 rpm. All the parameters of the radial bearings used are listed in Table 1.

Fig. 3 shows the position of the centres of the bearing journals centres in relation to the rotational speed. The lowest position of the journal corresponds to the lowest rotational speed of 2000 rpm. As the speed increases, the journal lifts in the bearing. The subsequent points have been connected to each other by straight lines. It can be noticed that the lines connecting the individual journal positions in the front bearing are quite irregular. During the analysis, temporary problems in achieving convergence of the calculations were noted at some speeds. This may indicate unfavourable conditions for the formation of a stable lubricating film. In practice, if the operation of the bearing is not stable, this situation should be improved by using an appropriately selected preload.

Fig. 4 shows the computationally obtained minimum thicknesses of the lubricating film for the two bearings. For the more heavily loaded front bearing, this parameter varied from 7 μm to 31 μm in the speed range from 2000 rpm to 20,000 rpm. The minimum thickness of the lubricating film in the less loaded bearing varied from 8 μm to 34 μm. At a nominal speed of 14,000 rpm, the minimum thickness of the lubricating film was 26 μm for the front bearing and 29 μm for the rear bearing. These values were deemed sufficient to ensure the proper operation of the bearings. The minimum lubricating film thicknesses obtained for the other bearings analysed were lower, which was one of the main premises for selecting the bearing variant discussed.

As part of the computational analysis, the theoretical lubricant demand of the bearings was also determined at different rotational speeds. Fig. 5 presents the results of this analysis for the more heavily loaded front bearing. As the speed increased, the lubricant demand of the bearing rose from 0.12 l/min at the lowest speed to nearly 2 l/min at 20,000 rpm. At the nominal speed, the flow rate of the low-boiling lubricant for the front bearing is 1.08 l/min. A similar flow rate value was obtained for the second bearing. At 14,000 rpm, the computationally determined friction losses are 1.12 kW in the front bearing and 1.04 kW in the less-loaded rear bearing. Given the dimensions and load of the bearings, the calculated friction losses can be considered low. This is related to the low viscosity of the lubricant.

The analysis of the stiffness and damping coefficients of the plain bearings in relation to the rotational speed allows the impact of the bearing characteristics on rotor dynamics to be assessed. In the Madyn 2000 program, bearing coefficients are calculated from a perturbation of the journal's equilibrium position, where the force resulting from the pressure distribution corresponds to the bearing load [38]. The computationally determined waveforms of the stiffness and damping coefficients of the bearings are shown in Fig. 6. Due to the design of the bearings, the stiffness and damping coefficients in mutually perpendicular directions are equal to each other. Therefore, for each bearing, the waveforms of these coefficients coincide with each other. The computationally obtained direct stiffness and damping coefficients of the two bearings initially decrease as the rotational speed increases to 12000 rpm. After exceeding this speed, the direct damping coefficients stabilise at around 30,000 N·s/m. With further increases in speed, the values of the direct stiffness coefficients change within a limited range (from $1.7{\cdot}10^7$ N/m to $4.0{\cdot}10^7$ N/m). The cross-coupled stiffness and damping coefficients reach values close to zero over the entire analysed range, which is characteristic of tilting pad bearings. Based on the presented calculation results, the decision was made to select the presented geometric variant of the bearing for further implementation. Before a prototype of this bearing was built, calculations were also made to check the dynamic properties of the rotor supported by the bearings in question, as discussed in the next subsection of the article.

Table 1
Radial bearing parameters used in calculations.

Parameter	Front bearing	Rear bearing
Bearing type	Tilting pad	Tilting pad
Number of pads	4	4
Pad configuration	According toFig. 2a	According toFig. 2a
Angular length of one pad	70°	70°
Journal diameter	70 mm	70 mm
Bearing width	45.7 mm	45.7 mm
Radial clearance	0.0525 mm	0.0525 mm
Bearing preload	0	0
Lubricant	Hexamethyldisiloxane (MM)	Hexamethyldisiloxane (MM)
Density of lubricant	726.86 kg/m^3 (60 °C)	726.86 kg/m^3 (60 °C)
Dynamic viscosity of lubricant	0.000335 N·s/m^2 (60 °C)	0.000335 N·s/m^2 (60 °C)
Static load	358 N	482 N

2.2. Analysis of the dynamic properties of the rotor

During the design process of the microturbine, both static and dynamic rotor calculations were performed that took into account the characteristics of the two radial support bearings discussed earlier. The FEM model of the complete rotor is shown in Fig. 7. The rotor model takes into account all the elements that affect the static and dynamic properties of the rotating system. In the case of a rotor disc, whose blade ring is not a solid body, substitute diameters were adopted to correctly represent the mass and moments of inertia of this component. In total, the rotor model consists of 40 Timoshenko-type beam elements with six degrees of freedom at each node. The total length of the rotor is 1035 mm, and the support bearing spacing is 651 mm. According to the developed model, the total mass of the rotor is 85.61 kg. The nominal rotational speed of the rotor is 14,000 rpm, which corresponds to a frequency of 233.33 Hz.

The results of the strength analysis confirmed that the normal and shear stresses in the cross sections of the shaft are at a very low level. The maximum reduced stresses reach a value of 6 MPa and occur at the section between the rotor disc of the microturbine and the front bearing. The main source of these stresses is the torque transmitted through the shaft from the rotor disc to the generator. The maximum static displacement of the shaft, which does not exceed 35 μm, occurs at the free end where the rotor disc is embedded.

The dynamic analysis of the rotor included simulation modal analysis and forced vibration analysis. As part of the simulation modal analysis, the bending and torsional vibrations of the rotor were determined up to a frequency of 500 Hz, which was more than twice the nominal rotational frequency. Calculations were performed for several rotational speeds, but only selected results obtained for the nominal speed are discussed in the article. In the frequency range limited to 500 Hz, the analysed system has six natural vibration modes:

- four lateral vibration modes in the frequency range from 100.6 Hz to 124.8 Hz, at which displacements of the unyielding shaft in the bearings are observed. These are the so-called cylindrical and conical vibration modes, which in this case are strongly damped (damping of more than 31%), so they should not significantly affect the dynamics of the rotor.
- two bending vibration modes at frequencies of 234.6 Hz (backward whirling) and 418.1 Hz (forward whirling). These natural vibration modes are shown in Fig. 8 and Fig. 9. Normally, bending vibration modes have a major impact on the dynamics of the rotor, but in the case discussed they occur outside the operating range, as the nominal

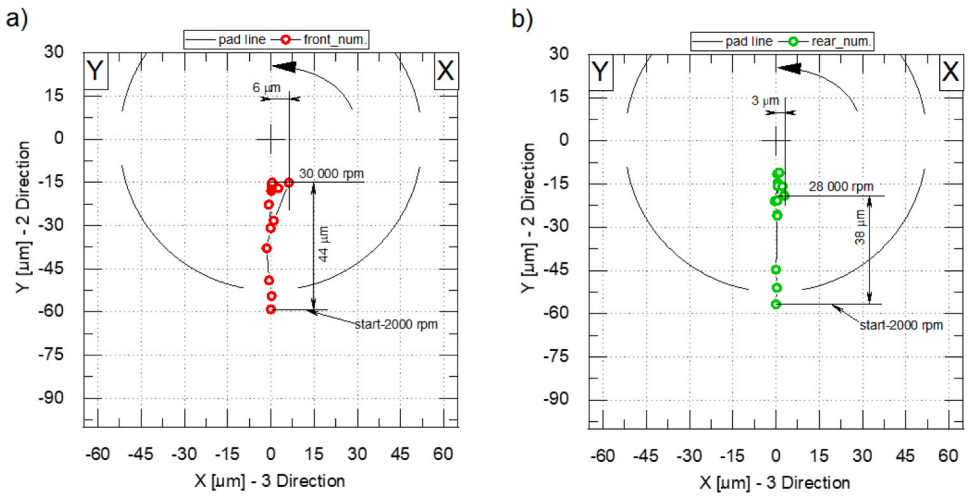

Fig. 3. The position of the centre of the journal in relation to the rotational speed (a – front bearing, b – rear bearing).

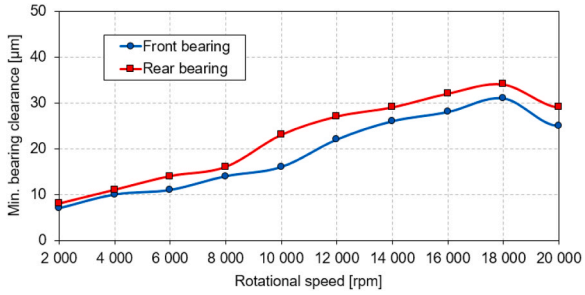

Fig. 4. The minimum height of the lubrication gap in two journal bearings lubricated with a low-boiling liquid medium.

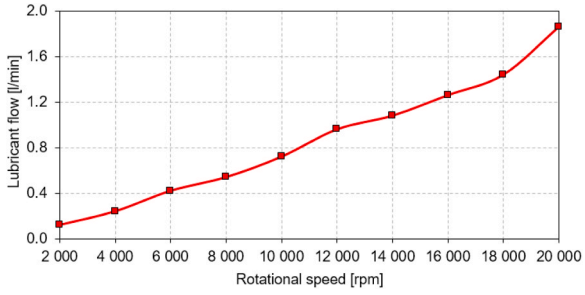

Fig. 5. Front bearing's demand for a lubricant in the form of a low-boiling liquid medium.

rotational speed is 14,000 rpm and these modes occur at 19,474 rpm and 25,088 rpm respectively.

- Additional analysis showed that the first torsional vibration mode of the rotor occurs in this case at a frequency of 508 Hz.

Based on the simulation modal analysis, the rotating system of the microturbine was found to be subcritical, meaning that the first bending vibration mode of the rotor occurs above the nominal rotational speed (which in this case is also the maximum speed).

In order to check the impact of individual natural vibration modes on rotor vibration during operation at different rotational speeds, the amplitude-phase characteristics of the rotating system were determined for different unbalance conditions. Calculations were performed assuming that the maximum permissible unbalance of the system (equal to about 200 g·mm for class G 2.5 according to the ISO1940–1 standard) would be modelled in three ways:

A. using one additional concentrated mass located in the central part of the rotor (near the centre of gravity),
B. using two additional concentrated masses located in the central part of the rotor and in the centre of the rotor disc,
C. using two additional concentrated masses located in the central part of the rotor and in the centre of the rotor disc, but the mass located on the rotor disc will be additionally rotated 180° relative to the mass located in the centre of the rotor.

All unbalance variants are represented graphically in Figs. 10–12 that show the vibration levels of individual rotor parts as a function of rotational speed. Below the nominal speed, the vibration level in all unbalance variants is low (not exceeding 12 µm), with the highest vibration level occurring for variant B. Above the nominal speed, the vibration level gradually increases. The highest vibration level occurs at a speed of approximately 27,500 rpm. This is related to the occurrence of the bending vibration mode shown in Fig. 9. The vibration level does not exceed 50 µm over the entire speed range analysed. Given the significantly lower vibration level in the operating speed range, the obtained results of the forced vibration analysis can be considered acceptable. At the nominal speed, the vibration level did not exceed 8 µm. The largest vibrations occurred at the rotor ends (on the rotor disc and thrust plate).

The Campbell diagram for the analysed rotor is shown in Fig. 13. On its basis, it can be concluded that when increasing the rotational speed, excitations can occur which will cause an excitation of selected vibration modes. In the case of an excitation whose frequency is in line with the rotational speed (1X), only the vibrations of the rotor as a rigid body will be excited below the nominal speed, which should not cause major problems due to their strong damping, exceeding 31%. Therefore, it can be concluded that rotor vibrations caused by an unbalance with a frequency matching the rotational frequency should not be a source of any instability. Transverse vibrations of the rotor can only be induced by excitations with a frequency that is a multiple of the rotational frequency. In the case of excitations such as 2X and 3X, an excitation of transverse vibrations will occur below the nominal speed, in the range of about 7000 rpm to about 12,000 rpm. To limit the vibration level in this speed range, the possibility of the appearance of superharmonic components during microturbine operation must be minimised. This should ensure stable rotor operation within the nominal speed range and below.

2.3. *Material selection for bearing segments*

The next stage of work on the new tilting pad bearings was a material

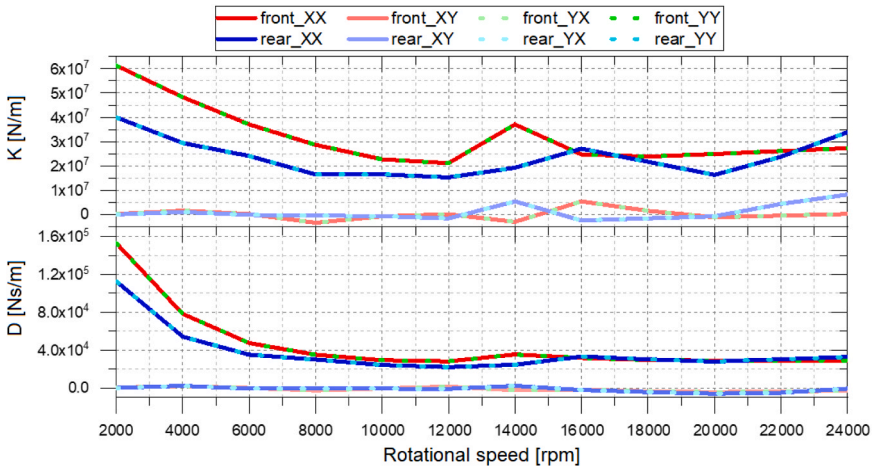

Fig. 6. Stiffness and damping coefficients of two journal bearings lubricated with a low-boiling medium.

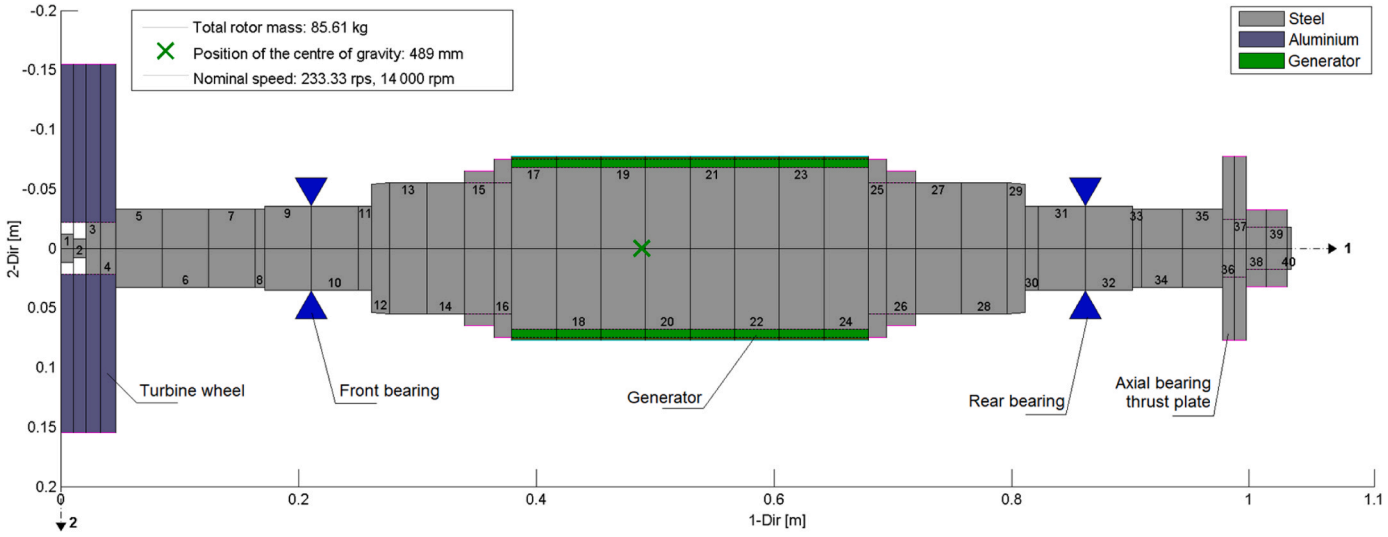

Fig. 7. FEM model of the 300 kW ORC microturbine rotor.

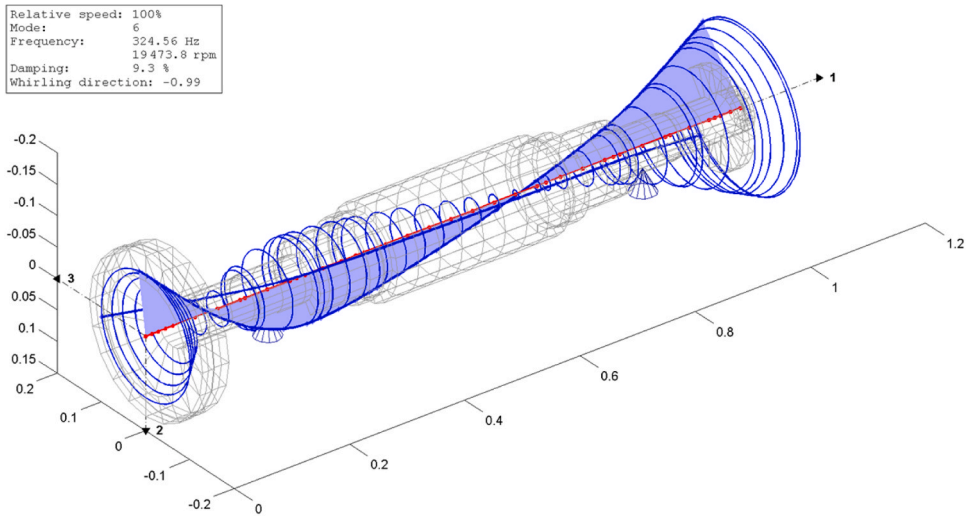

Fig. 8. Bending vibration mode of the microturbine rotor (backward whirling) at a frequency of 324.6 Hz.

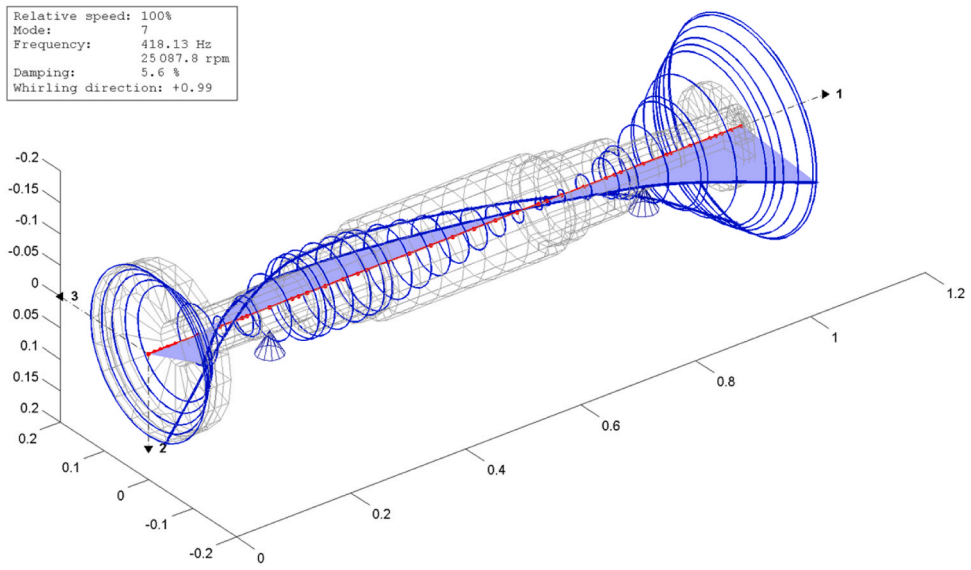

Fig. 9. Bending vibration mode of the microturbine rotor (forward whirling) at a frequency of 418.1 Hz.

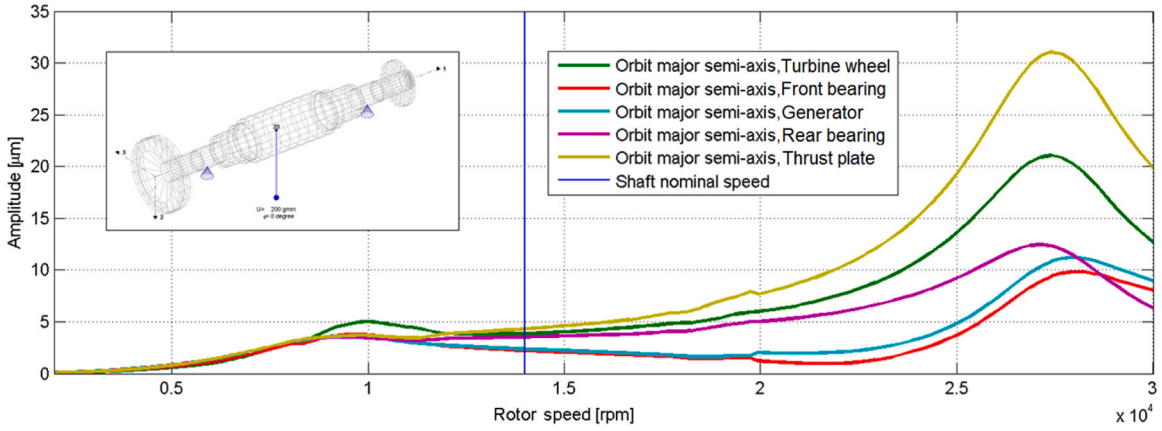

Fig. 10. Forced vibration of the rotor due to unbalance (according to variant A).

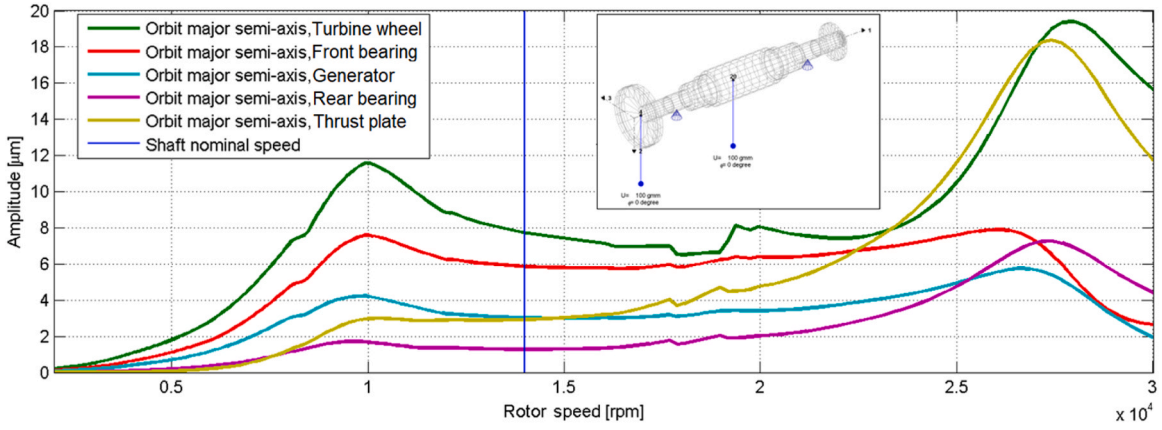

Fig. 11. Forced vibration of the rotor due to unbalance (according to variant B).

selection for their sliding surfaces. The use of bearings lubricated with coolant, which has a significantly lower viscosity and lubricity compared to oil, forced the use of special design solutions and unconventional sliding materials capable of being lubricated with toluene. Due to the requirements related to the operating conditions of the bearings, the range of materials that could be used was very limited. Temperatures above 100 °C that could occur in the turbine excluded the use of classic bearing alloys based on white metal. Compatibility with working fluids used in the ORC microturbine was another limitation. Three groups of materials were considered: bronze bearings with the

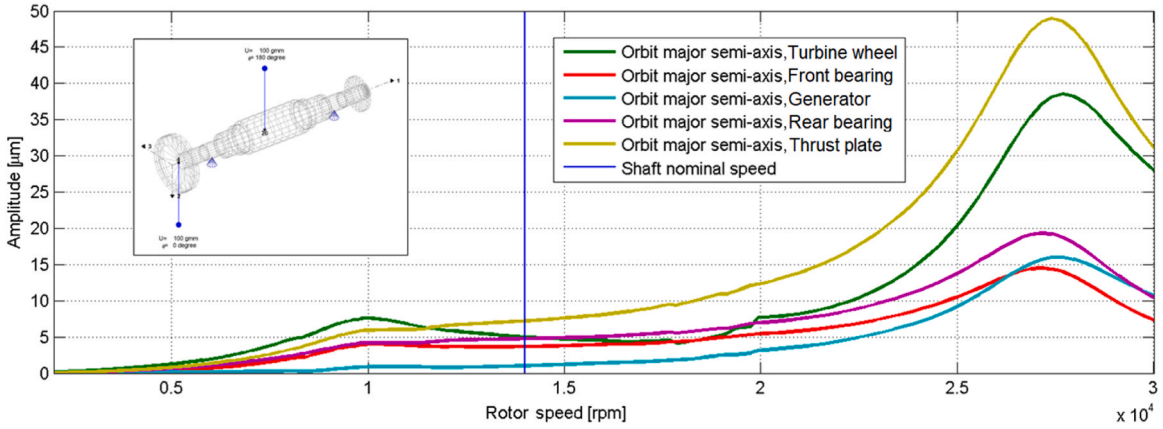

Fig. 12. Forced vibration of the rotor due to unbalance (according to variant C).

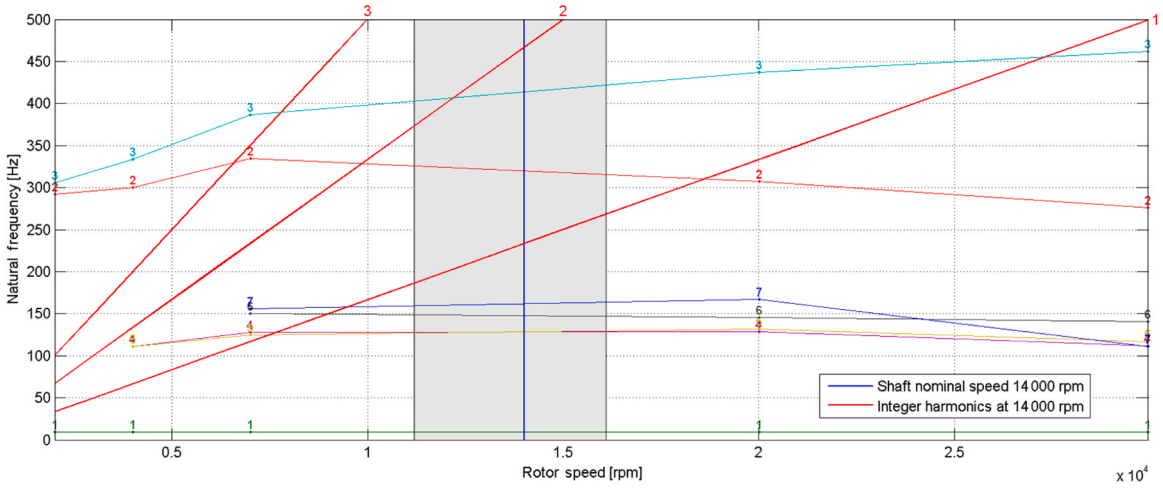

Fig. 13. Campbell diagram in the speed range up to 3000 rpm and frequency range up to 500 Hz.

addition of graphite, ceramic materials (ultimately rejected due to high brittleness) and specialized plastics (PEEK, PAEK, PPS) [39,40].

During the tests of PEEK-based materials as part of the project funded by the National Science Centre, PEEK with the addition of graphite and carbon fibre displayed excellent tribological properties [39,40] and performed well in the conditions of lubrication with low-viscosity liquids, even when the coefficient determined as the product of the nominal pressure and the peripheral velocity reached up to 15 MPa·m/s. Examples of samples after testing on a tribometer are shown in Fig. 14.

Favourable test results of the material, in combination with other beneficial properties such as deficient absorption, the possibility of continuous operation up to 250 °C, good mechanical properties, and high dimensional stability during machining, have led to its selection for the segments of the designed bearing.

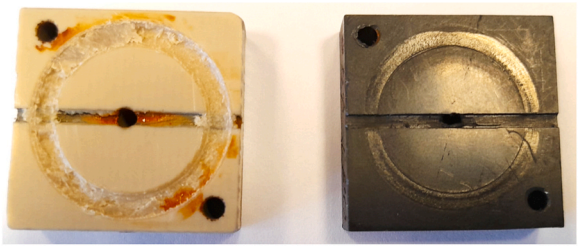

Fig. 14. Appearance of samples after testing – PEEK natural (beige) and PEEK CF30 with additives (black) after analogous tribometer tests.

2.4. Design of prototype tilting pad bearings

As described in the previous parts of the article, the rotor was supported laterally on 4-segment tilting pad bearings. During the design of the radial bearings, two main technical problems were encountered:

- The problem of choosing the best sliding material and determining the method of its attachment to the sliding segments.
- The problem of obtaining the desired sliding geometry and bearing clearance within the resultant tolerance of ± 0.01 mm,

Choosing the right sliding material was discussed in the previous section of the article. The second problem has been solved by introducing a special adjustment mechanism that allows adjusting the distance of the segments to the journal, described in more detail in an earlier publication [41–43].

In modern plain bearings, the classic sliding layer made of poured white metal is increasingly often replaced with a polymer sliding layer. It has many advantages when lubricated with liquids of low viscosity and low lubricity because the structure of polymers and the additives contained within them improve their tribological properties. Of course, polymer sliding layers also have numerous disadvantages and limitations, such as low thermal resistance, water absorption, low stiffness which makes accurate machining difficult, poor heat dissipation, etc.

The literature and previous research by the authors reveal that the polymer layer of the hydrodynamic radial bearing should not be excessively thick. This is due to the fact that polymer materials have a

much higher coefficient of thermal expansion and at the same time much lower stiffness compared to classic sliding layers (white metal). As a result, the thick polymer layer undergoes unfavourable deformations under the action of hydrodynamic pressure and temperature, which reduce the load capacity of the bearings and increase their wear. "Swelling" of the sliding layer under the influence of temperature can also lead to a reduction of bearing clearance, and consequently to its destruction. In addition, the much lower mechanical strength and stiffness of polymers compared to steel precludes the use of monolithic sliding segments in heavily loaded bearings, because they would undergo too much deformation, changing the shape of the lubrication gap.

Currently, the most common method of attaching a polymer sliding layer to a steel base is hot pressing the polymer layer into the steel. In order to increase the bonding strength of the polymer to the steel base, special technologies are developed for coating it with an intermediate layer of bronze, imprinting dimples or welding a steel mesh to the surface. The method of hot fixing of polymers is energy-intensive, expensive, and does not allow regeneration of the sliding layer. Another known method of attaching the polymer layer to the steel base of the flat segment of a thrust bearing is the use of a trapezoid-shaped pocket secured from the outside with a locking plate [44]. However, this solution is intended for thrust bearings, in which the sliding elements are flat. Moreover, it does not guarantee the adherence of the polymer to the steel over the entire surface. Also known is the solution, in which the polymer layer is attached to the bearing housing only along the trailing edge, in which there are areas with locally reduced stiffness selected with a computer simulation, in the form of cavities fully filled with material (e.g. rubber, polyurethane or other flexible material) of a significantly lower stiffness with respect to the housing material [45].

Due to the fact that in existing bearing solutions there had been no satisfactory method of attaching a polymer sliding layer to a steel segment, the authors have developed their own original solution, which has been submitted for patent. In a segment with a polymer layer designed according to the invention, the polymer layer is stably fixed in the steel segment by means of a dovetail-shaped connection (Fig. 15). This polymer component can be easily assembled by sliding it into the steel sleeve and securing it with side screws. It is then clamped with a flexible lip deformed with screws. In addition, the polymer layer can be secured against sliding out by means of a radial pin or screw. Independently from the shaped connection and the locking lip, the polymer piece can additionally/alternatively be glued to the segment. For this purpose, the design can feature one or more circumferential grooves containing the glue connecting the polymer piece with the segment. The adhesive can be applied before assembly or pressed into the groove after the segment has been fitted. In addition to a single bearing segment with a polymer component attached, Fig. 15 also shows a complete journal bearing. Two such bearings were used to support the microturbine shaft, as shown in Fig. 1.

Since the microturbine rotor must also be supported in the axial direction, the project resulted in developing a special thrust bearing design with spray nozzles between its segments and a flexible housing support to compensate for seat manufacturing errors and thermal deformation of the microturbine. A complete thrust bearing with segments made of the same sliding material as in the radial bearings is shown in Fig. 16. The same bearing will maintain forces in two axial directions in the ORC microturbine.

3. Experimental studies

3.1. Characteristics of the ORC microturbine and test rig

The ORC system, for which the prototype turbogenerator is designed, is capable of efficient operation in two modes: condensation mode (preferred during the summer season) and cogeneration mode (optimal during the winter season). After passing through the evaporator, the working medium of the ORC power plant (MM – hexamethyldisiloxane) reaches a temperature of about 190 °C and a pressure of about 700 kPa (a). In the condensation mode, the condenser of the ORC power plant is cooled using a fan cooler. In the cogeneration mode, on the other hand, the heat from the condenser is used for heating purposes, which involves raising the condensation pressure and temperature.

Within the framework of the project, a decision was made to implement a single-stage impulse turbine. This decision was dictated by the ability to achieve satisfactory efficiency while minimising the axial force and the lift-up speed of the rotor, all while maintaining a simple design. The nominal speed during operation in the cogeneration mode is lower than in the condensation mode, decreasing from 14,000 rpm to 12,000 rpm. The maximum power of the turbogenerator in the condensation mode is approximately 300 kW. The flow system of the microturbine was subjected to multi-criteria shape optimisation, which made it possible to optimise the turbine's internal efficiency in both the condensation and cogeneration modes. As a result, the optimised turbine stage achieves an efficiency of approximately 76.7% in the condensation mode and 77.8% in the cogeneration mode. A detailed description of the optimisation methodology is presented in the article [46].

Tests on prototype plain bearings lubricated with a low-boiling liquid medium were carried out at the laboratory of the Institute of Fluid-Flow Machinery of the Polish Academy of Sciences (IMP PAN), located in Gdańsk. A prototype microturbine, for which the bearings were designed, served as a test rig for the bearings. Thanks to such an approach, the bearings were tested under conditions similar to the target operating conditions. The microturbine was placed on a steel frame. An auxiliary system was built to supply the bearings, which included a working liquid pump, tank, cooler, and control system. Lubricant flow and pressure were adjusted independently for each bearing. The flow rate and pressure of the lubricating medium were adjusted separately for each bearing. During the bearing tests, the microturbine rotor disc was driven by compressed air at an elevated temperature. The dynamic state of the machine was monitored using Dewesoft's data acquisition system (IOlite), which was connected to the following types of sensors:

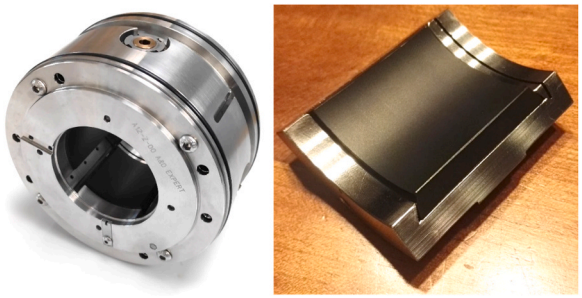

Fig. 15. Prototype tilting pad radial bearing with sliding surfaces made of polymer material (on the left – a complete bearing, on the right – one tilting pad wth polymeric material).

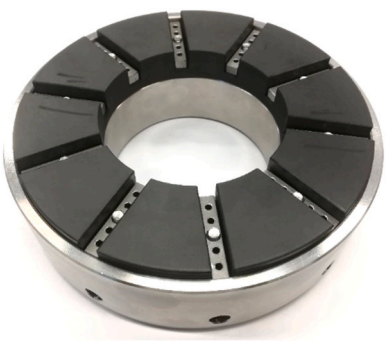

Fig. 16. Prototype thrust bearing with sliding pads made of polymer material.

- uniaxial accelerometers (2 accelerometers were used to measure vibration in the radial direction on each bearing and 1 accelerometer was used to measure vibration in the axial direction),
- 7 eddy current sensors, the arrangement of which is shown in Fig. 17 (4 sensors were used to measure displacements in the radial direction, 1 sensor to measure displacements in the axial direction, 1 sensor served as a phase sensor and 1 sensor served as a shaft speed sensor),
- 8 J-type thermocouples (which were used for monitoring bearing temperature).

The arrangement of the sensors on the prototype microturbine is shown in Fig. 18. They are organised into groups based on their assigned colours. Accelerometers are marked in blue, eddy current displacement sensors in red, speed sensors in purple and temperature sensors in green. Two eddy current sensors each were placed near the front bearing (which is situated close to the vapour inlet of the microturbine) and the rear bearing (which is located in the rear part of the machine). The sensors were rotated by 90° relative to each other and by 45 ° relative to the horizontal plane. Two eddy current sensors were placed in the axial direction in the rear cover of the casing to measure the displacement and rotational speed of the shaft. One eddy current sensor was mounted in the vertical direction at the upper rear part of the casing to measure the phase angle. In the radial bearings, one thermocouple was installed at each pad (Front_B-temp, Rear_B-temp). In addition, 4 temperature sensors were placed in the axial, more heavily loaded bearing (A_B_front) and 2 thermocouples in the less heavily loaded bearing (A_B_rear). Two accelerometers were installed in the plane of the radial bearings (in the horizontal direction) and one was installed on the rear cover in the axial direction. Such a set of sensors allows for the measurement of all the most important parameters on the basis of which the proper operation of both the bearings and the microturbine can be assessed.

3.2. Results of experimental studies

The experimental study of the prototype microturbine involved conducting numerous series of measurements to determine various characteristics of this machine. This part of the article discusses selected results of the experimental study, which concern the bearing system and rotor dynamics. That covered measurements of temperatures in the bearings, the displacements of bearing journals and the vibration amplitude of the shaft, which were conducted at various rotational speeds. In addition, the vibration trajectories of the bearing journals were measured at selected rotational speeds. The selected results of the experimental study were compared with previously discussed calculation results. During this research, the flow system of the microturbine was supplied with hot air, but all the bearings were supplied with the target lubricating medium—a low-boiling medium in liquid form (MM).

Fig. 19 shows the temperature waveforms measured in the bearings during a gradual increase in rotational speed, first to 9277 rpm and then to 12,700 rpm. At a speed of 9277 rpm, the rotor ran for six minutes. After the speed was increased to 12,700 rpm, the rotor continued to run at this higher speed for four minutes. In Fig. 19, the black line shows the course of rotational speed. The temperature waveforms in the two journal bearings were similar to each other, but the temperature in the front bearing was about 2–3 °C higher over almost the entire range tested. The highest recorded temperature in the front bearing was 47 °C and occurred at the end of the tests conducted with the highest speed. In the front axial bearing, the highest temperature was 58 °C and was noted in the lower part of the bearing. In the upper part of this bearing, the temperature reached 50 °C. In the rear axial bearing, the maximum temperature was 45 °C and it also occurred in the lower part of the bearing. The results of the temperature measurement in the upper part of the rear bearing showed abnormal lubrication. It was concluded that the lubricating medium was not being supplied to the upper part of the bearing due to the distance between the sliding segments and the thrust plate being too large. Under such conditions, the lubricating medium supplied to the bearing was not evenly distributed to all segments and flowed to the outlet due to gravity. It should be added that the phase transformation temperature of the lubricating medium at atmospheric pressure is approximately 80 °C. Based on the results of the temperature measurement of the sliding pads, it can therefore be thought that there should be no evaporation of the lubricating medium anywhere inside the bearing.

To mitigate the risk of MM lubricant evaporation during extended bearing operation, additional measures to prevent temperature rise have been implemented. Firstly, an additional cooling system for the bearing lubricant is provided, activating when the temperature exceeds 65 °C. Since during the tests, the results of which are shown in Fig. 19, the temperature did not exceed 65 °C, the additional cooling system was not used. If the bearing temperature reaches 80 °C, even after the additional lubricant cooling system has already been activated, the microturbine's control and measurement system automatically closes the supply valve located at the microturbine inlet, resulting in the shutdown of the microturbine. These safeguards are designed to prevent any damage to the bearings and the microturbine during prolonged operation.

Fig. 20 shows the displacements of the bearing journals during the microturbine run-up. Solid lines indicate the movements of the journals

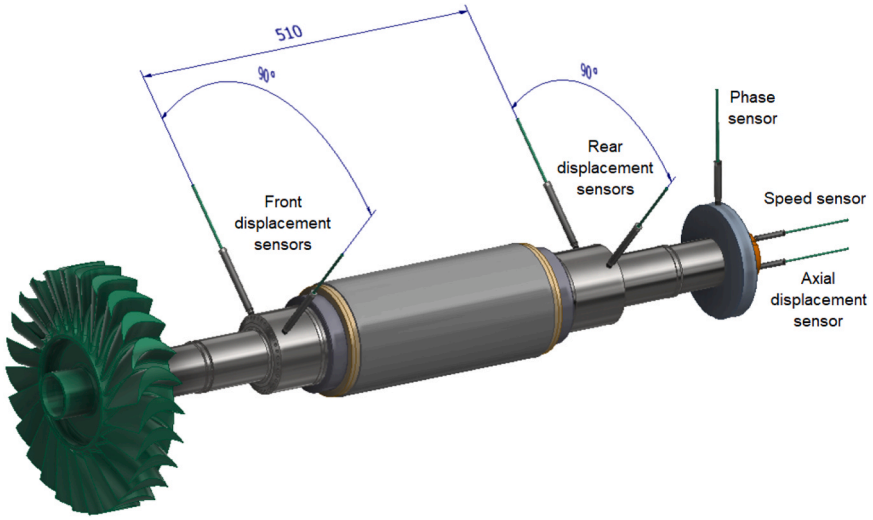

Fig. 17. Arrangement of eddy current sensors within the microturbine rotor.

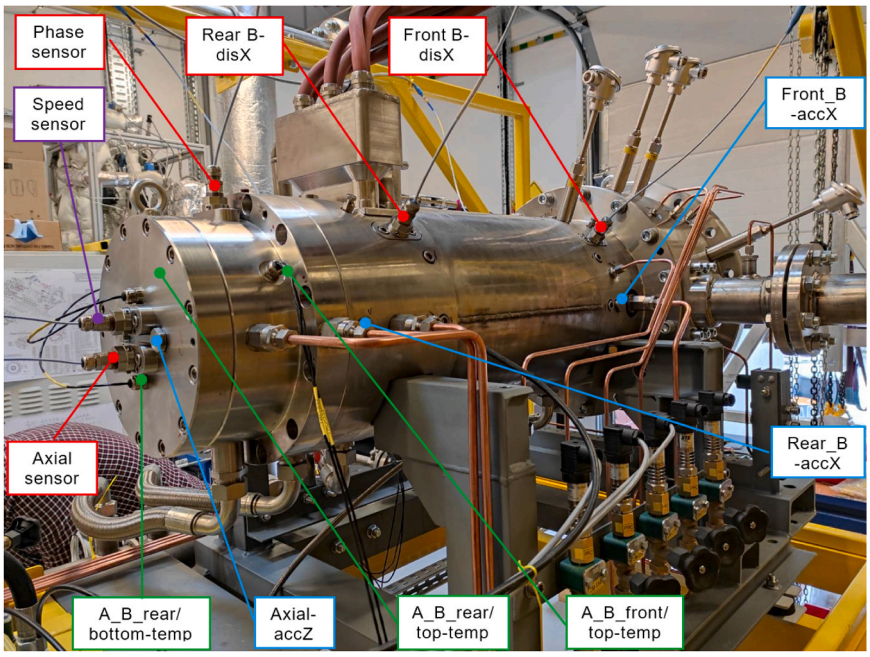

Fig. 18. Arrangement of sensors on the microturbine (photo taken from the side of the rear bearing).

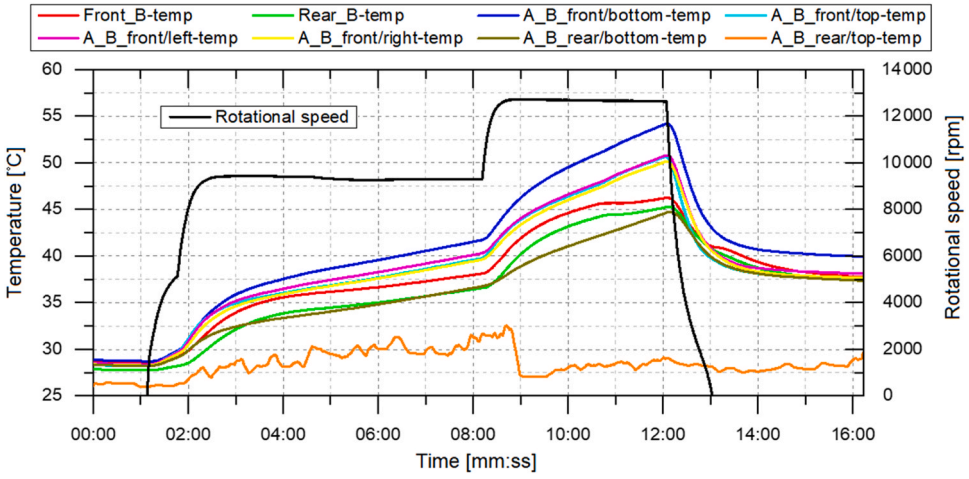

Fig. 19. Temperature waveforms in the radial and axial bearings of the microturbine.

within the lubrication space. In addition, the results of the numerical calculations, which are marked with points corresponding to specified rotational speeds, are included in the same diagrams. It was determined that the bearing radial clearance of 0.0525 mm could have increased to 0.135 mm with the maximum deflection of the pads. The maximum displacement of the journal centre was measured with the shaft resting in the bearings and without the supply of lubricating medium to the bearings. During start-up, as the speed increases, the bearing journals move towards the centre of the sleeve due to hydrodynamic pressure. Additionally, due to the rotational motion of the journal, they also move in the horizontal direction. At the maximum rotational speed, the rear bearing journal soared by approximately 71 μm, while the front bearing journal soared by approximately 68 μm. The differences are due to the higher static load of the front bearing. The experimentally obtained displacements of the bearing journals were of a similar nature to the displacements obtained by numerical calculations. The experimentally obtained displacements of the journal centre in the first bearing are greater than those determined theoretically. In the rear bearing, even at the lowest speed, these differences are not so great. As the rotational speed increases, the differences between the numerically and experimentally determined positions of the journal centre become smaller and smaller. At 12 krpm, the discrepancies between the model and the real object are the smallest. The observed differences between the results of the theoretical calculations and the experimental tests arise from the peculiarities of the two different methods used to determine them. It is worth noting that the theoretical model does not consider a number of factors that worsen the conditions for the formation of a stable lubricating film in a plain bearing. These factors include the non-parallelism of the journal and sleeve, inaccuracies in the manufacture of the sliding surfaces, and the dynamic load acting on the journal due to the residual unbalance of the shaft and the flow of the working medium in the microturbine. These factors could have caused the calculation results to appear more optimistic than the experimental results, which is particularly noticeable at lower speeds.

During the experimental research being discussed, the journal bearings were supplied with a lubricating medium at a volumetric flow rate of 2.8 l/min, while the thrust bearings received a lubricating medium at a volumetric flow rate of 3.5 l/min. Previously conducted

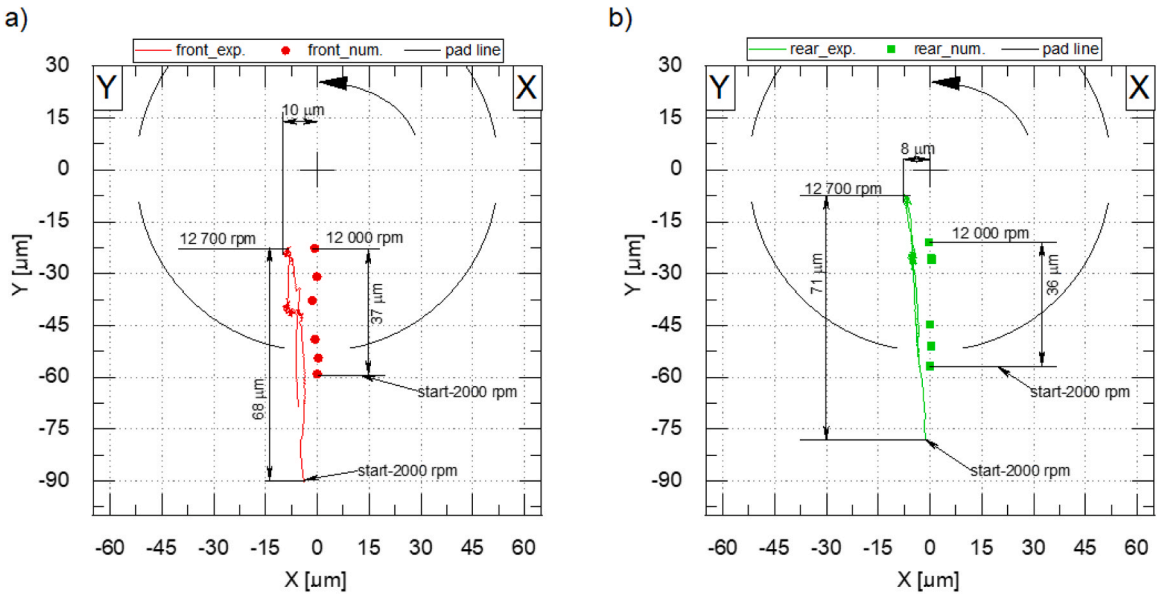

Fig. 20. Displacements of bearing journals as a function of rotational speed (a – front bearing journal, b – rear bearing journal).

numerical calculations showed a lower bearing demand for a lubricating medium, and the increased flow rate was intended to dissipate heat better and protect the bearings from rapid wear.

Fig. 21 shows the vibration waveforms of the bearing journals as a function of rotational speed. The results of experimental research (thicker lines with square markers) and numerical calculations (thinner lines with circular markers) are juxtaposed in a single graph. The red and green colours indicate the vibration of the front bearing journal in two mutually perpendicular directions. The vibration of the rear bearing journal was marked in the same way, using other colours, specifically navy blue and blue. During the experimental research, the rotor reached a maximum speed of 12,730 rpm, and the calculation results were presented over a wider range, up to 20,000 rpm. The results of experimental results showed that at higher speeds (above 7000 rpm), the vibration amplitude of the front bearing journal is greater than the vibration amplitude of the real bearing journal. The measured maximum vibration amplitudes in this bearing in the two directions did not exceed a value of 8 µm. The maximum vibration amplitudes measured in the rear bearing were lower, reaching 5 µm at 12,730 rpm. Within the range of 7000 rpm to 12,730 rpm, the vibration amplitudes in this bearing varied over a small range. At lower speeds, the vibration in this bearing increased as the speed increased. As in the earlier case, similar levels of displacement were recorded in the two directions. The results of experimental research confirmed that the prototype microturbine with atypical plain bearings operated correctly throughout the entire range of rotational speeds examined.

The displacements of the bearing journals obtained numerically are lower than the experimental values, but they have a similar course, particularly for the rear bearing journal. The differences between the calculation results and experimental results may have been due to the simplification of the model in comparison to the real object. As a result of factors such as geometrical inaccuracies in the actual bearing, variations in temperature and viscosity of the lubricating medium, or momentary changes in load, the computationally determined characteristics of the bearings may have differed from the actual ones. The results presented in Fig. 21 are strongly influenced by the residual unbalance. Three different rotor unbalance variants were analysed in the calculation method, but the mass distribution of the actual rotor may have deviated from them, which may have caused a change in the value and location of the dynamic force stemming from the unbalance. Despite the observed differences between the experimental and simulation research results, it can be recognised that the developed model of the

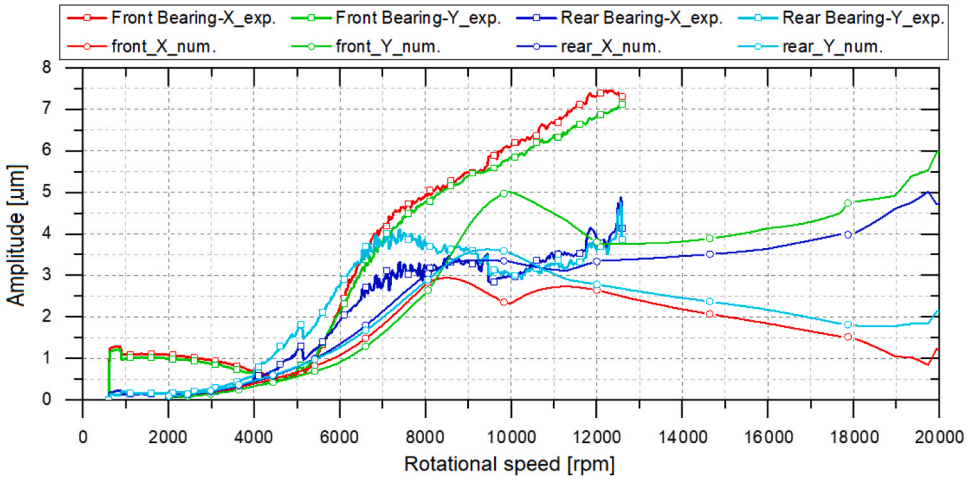

Fig. 21. Displacements of bearing journals in two mutually perpendicular directions obtained numerically and experimentally.

rotating system largely reflects the behaviour of the actual machine. In the rear bearing, the vibration level of the journal was predicted with satisfactory accuracy. The speeds at which the increases in vibration amplitude of the bearing journals occurred were also very well predicted. It can therefore be concluded that the applied model of the rotor with tilting pad bearings, lubricated with a low-boiling medium in liquid form, proved to be a very useful computational tool and allowed a preliminary determination of the characteristics of the rotating system.

Within the framework of the experimental research, the vibration trajectories of the bearing journals were also measured at different rotational speeds. Figs. 22–24 show the vibration trajectories of the journals at three selected speeds: 8000 rpm, 10,000 rpm and 12,000 rpm, respectively. The raw (unfiltered) signal from the displacement sensors is represented by the black curve. The trajectories after filtering to 1X (rotational frequency) have been marked in red. The displacements that occurred at a frequency of 4X are marked in green. Since this frequency component was apparent over almost the entire operating range of the microturbine. The shape of the unfiltered vibration trajectories of the journals results from the design of the bearings, wherein the journal moves within the lubrication gap between the four tilting pads. A similar phenomenon was observed and described in the work [47], where the shape of the vibration trajectory changed depending on the number of tilting pads and the direction of the acting load. After applying the filter, it is noticeable that in the front bearing vibrations associated with the rotational speed (1X) gradually increase with increasing speed, whereas in the rear bearing, the vibration amplitude varies over a small range. In both bearings, it can also be noticed that the rotational speed has some influence on the shape of the 1X vibration trajectory. The vibration at a frequency of 4X takes place in the vertical direction, with almost zero horizontal displacement. In the vertical direction, the amplitudes of the vibrations with a frequency of 4X turned out to be higher compared to those at a frequency of 1X.

At a speed of 8000 rpm, the maximum peak-to-peak (p-p) vibration amplitude in the front bearing is 25 μm (with an RMS value of 8.8), and in the rear bearing 22 μm (with an RMS value of 7.8 μm), as can be seen in Fig. 22. The vibration amplitude of the front bearing journal at 1X is 10 μm, while the vibration amplitude of the rear bearing journal is 8 μm. According to the ISO 10816–3 standard, the vibrations of the bearing journals are well below the permissible level. For large machines in the power range of 15–300 kW, the permissible RMS vibration level is 22 μm. It means that the vibration amplitudes of the bearing journals reached less than half of the recommended maximum value, which is fully acceptable.

Fig. 23 shows the vibration trajectories of both journals at a rotational speed of 10,000 rpm. The unfiltered vibration trajectories become separated, with a peak-to-peak (p-p) vibration amplitude of 27 μm in the front bearing and 24 μm in the rear bearing. The maximum vibration amplitude at 1X reaches 12 μm in the front bearing and is almost equal to the amplitude at 4X. In the rear bearing, the vibration amplitude at 1X is 5 μm and in this bearing, it is two times lower than the vibration amplitude observed at a frequency four times higher.

Fig. 24 shows the vibration trajectories of both journals at a rotational speed of 12,000 rpm. The vibration trajectories plotted on the basis of the unfiltered signal have an irregular shape, similar to the trajectory obtained at 10,000 rpm. The peak-to-peak (p-p) vibration amplitude is 30 μm in the front bearing and 25 μm in the rear bearing. The vibration trajectory of the front bearing journal after filtering to a frequency of 1X has a regular shape that is similar to a circle with diameter of 15 μm. In the rear bearing, it is smaller and its shape is similar to an ellipse with a vertically positioned major axis. The vibration amplitude in this case is 8 μm. It can also be noted that the major axes of the elliptical trajectories obtained for the two bearings are inclined at different angles. The presence of multiple harmonics in the vibration spectrum can have various causes. Separate publications are devoted to this issue. In the work [48], the authors suggest that the appearance of higher-order harmonics may signal the dissipation of the energy of irregular vibrations associated with the periodic rubbing of two bearing surfaces against each other. The authors of the next publication on this subject [49] investigated the vibration level of the bearing journal depending on pad wear. Their research showed that pad wear has a significant impact on the vibration of the rotor–bearing system, which confirms the necessity for current monitoring of the dynamic state of these types of bearings. In the case of the microturbine in question, however, there were no unequivocal symptoms indicating a break in the lubricating film and damage to the sliding surfaces of the bearings. Based on the measurement results, it can be assumed that there was no rubbing of the journal against the pads during the operation of the system. This was confirmed by a visual inspection of the bearing sliding surfaces conducted after the tests were completed. Visual assessment of the surface quality of the bearings revealed that the original machining marks from the manufacturing process were visible across the entire sliding surface of the pads and journal. When the image was zoomed in,

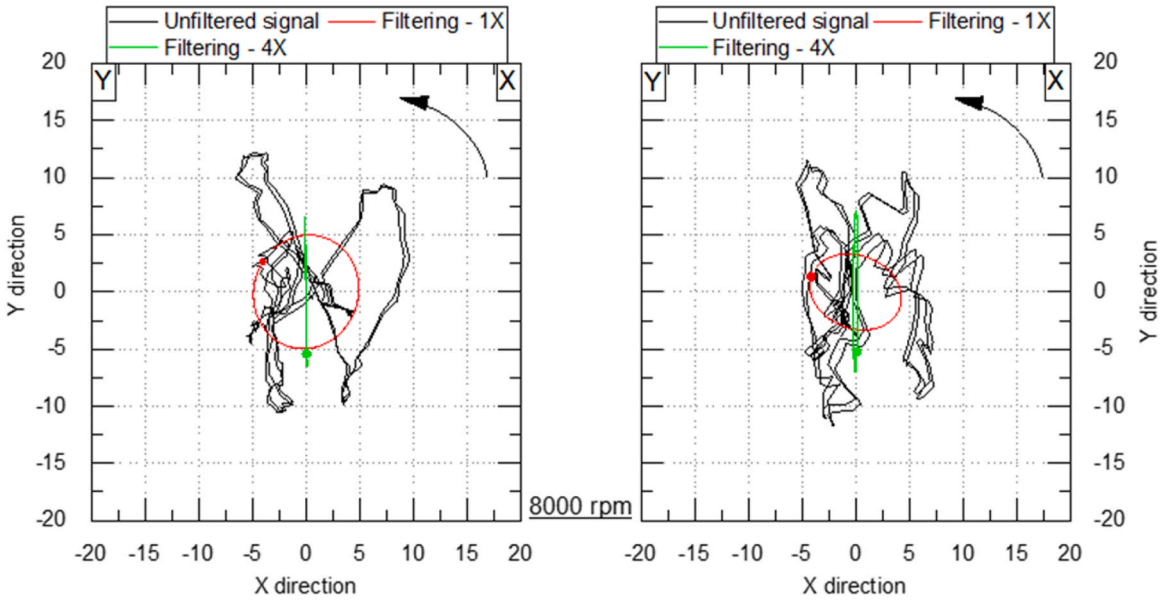

Fig. 22. Vibration trajectories of bearing journals at a speed of 8000 rpm.

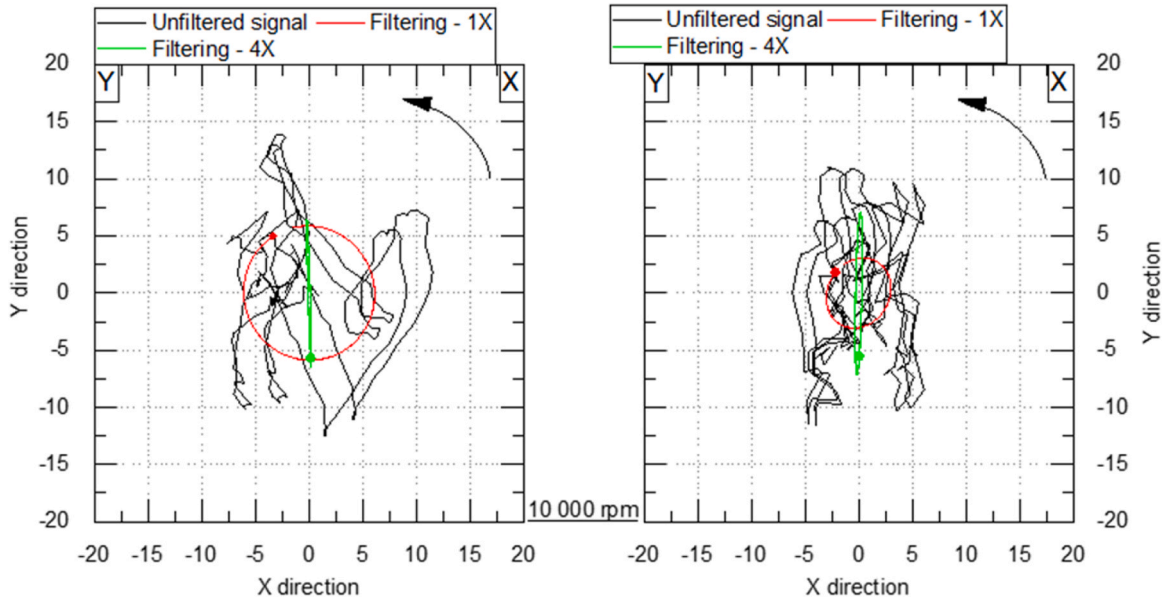

Fig. 23. Vibration trajectories of bearing journals at a speed of 10,000 rpm.

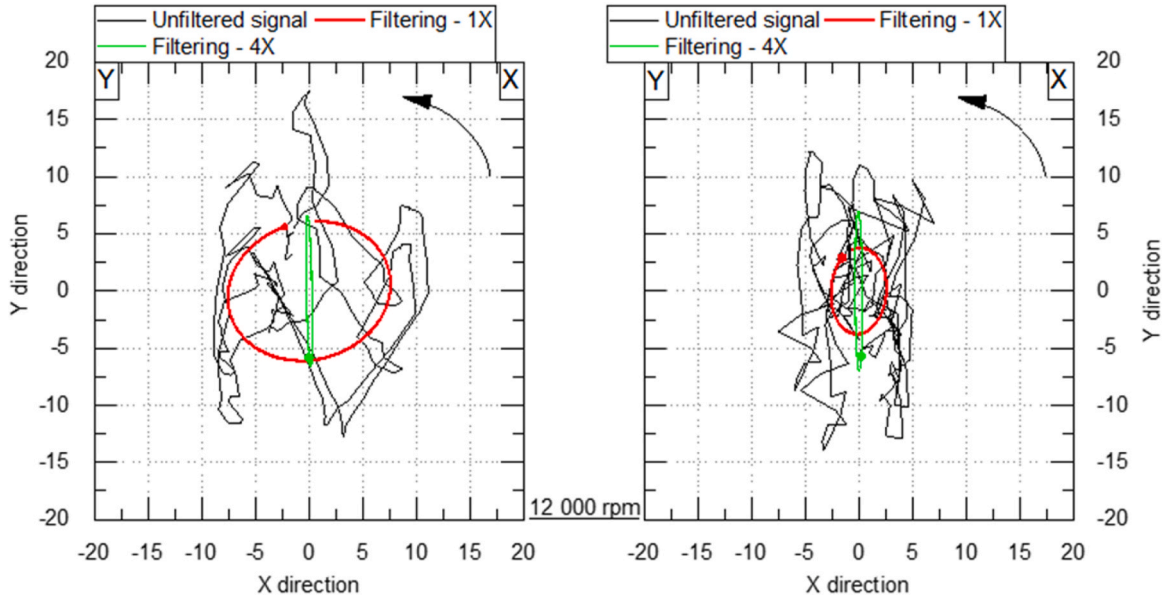

Fig. 24. Vibration trajectories of bearing journals at a speed of 12,000 rpm.

small traces of bearing lapping were visible on the tops of the bumps, which is normal and fully acceptable.

In all the cases discussed, concurrent vibrations of the bearing journals were observed, so they moved along a vibration trajectory in line with the direction of rotation. Throughout the entire operating range of the microturbine examined, the phase marker had a similar angular position in both bearings. This confirmed the results of earlier numerical analyses, which indicated that below the nominal speed, the rotating shaft line takes a cylindrical or slightly conical shape.

4. Conclusions

The article discusses numerical calculations and experimental research conducted on an innovative bearing system designed for an ORC microturbine. The innovation of the proposed design solution for the bearings lies in the use of tilting pads with sliding surfaces made of a high-temperature-resistant plastic. In addition, these bearings are lubricated with a low-boiling medium in liquid form. The numerical analyses included the determination of the basic characteristics of the bearings and the selection of chosen geometrical parameters. Within the framework of experimental research, tests were conducted on the microturbine with prototype bearings at different rotational speeds. The results of the experimental research were compared with the results of the calculations, which confirmed the correctness of the method adopted for modelling the rotor–bearing system. The experimental studies also confirmed the correct operation of the bearings under very difficult conditions—when lubricated with a low-viscosity liquid.

The experimental research results showed that the dominant vibration components were 1X and 4X. The 4X component, present over almost the entire range of rotational speeds, was found to be associated with the cyclical movement of the journal between the four tilting pads. It also stems from the vibration analysis of the journals that a low-

amplitude 0.5X subsynchronous component that appeared at higher rotational speeds could be a sign of lubricating film instability. This instability can be associated with the turbulences present in the lubricating film, as the lubricating medium used has a very low viscosity, which further decreases with increasing temperature. Despite the occurrence of additional components in the vibration spectrum, the overall vibration level of the bearing journals—according to the ISO 20816–3 standard—was low and the microturbine was able to operate without any operational limitations.

The chosen type of plain bearing with polymer tilting pads, where a low-boiling medium in liquid form was used for lubrication, was found to be suitable for use in the examined ORC microturbine. The use of such bearings has a beneficial effect on the vibration level and ensures stable rotor operation over a wide range of rotational speeds. Despite its low viscosity, the chosen lubricating medium, used in a bearing with the proper design and materials, successfully performed its role. The presented investigations have confirmed that the bearing system used holds great promise for high-speed turbomachines. The obtained research results, therefore, open up new possibilities in designing bearing systems for heavy microturbine rotors. In further works concerning this bearing system, attempts will be made to use different values of preload and assess the impact of this parameter on the static and dynamic characteristics of a turbomachine. Long-term tests of the developed bearings at elevated temperatures, which may result in local deformations of the polymer components, are also planned in a subsequent study. Future work will also include testing the possibility of using other low-boiling mediums for bearing lubrication.

Declaration of Competing Interest

The authors declare that they have no known competing financial interests or personal relationships that could have appeared to influence the work reported in this paper.

Data Availability

Data will be made available on request.

Acknowledgement

The presented research has been conducted as part of the POIR.01.01.01–00-0414/17 project titled “Development of the first Polish prototype mediumpower 300 kW ORC generator using industrial waste heat” co-financed by the European Union from The European Regional Development Fund and executed by MARANI Sp. z o.o. The National Science Centre (Poland) supported the work on the material selection for bearing segments [grant number 2019/35/N/ST8/03313].

References

[1] Wieland C, Schifflechner C, Braimakis K, et al. Innovations for organic Rankine cycle power systems: current trends and future perspectives. Appl Therm Eng 2023; 225:120201. https://doi.org/10.1016/j.applthermaleng.2023.120201.
[2] Mariani A, Laiso D, Morrone B, Unich A. Exergy analysis of organic Rankine cycles with zeotropic working fluids. FDMP-Fluid Dyn Mater Process 2023;19(3): 593–601. https://doi.org/10.32604/fdmp.2022.022524.
[3] Daniarta S, Nems M, Kolasinski P. A review on thermal energy storage applicable for low- and medium-temperature organic Rankine cycle. Energy 2023;278(A): 127931. https://doi.org/10.1016/j.energy.2023.127931.
[4] Phli R, Wieland C, Spliethoff H, Haglind F. Optimal tuning of model predictive controllers for organic Rankine cycle systems recovering waste heat from heavy-duty vehicles. Appl Therm Eng 2022;220:119803. https://doi.org/10.1016/j.applthermaleng.2022.119803.
[5] Mago P, Luck R. Energetic and exergetic analysis of waste heat recovery from a microturbine using organic Rankine cycles. Int J Energy Res 2013;37(8):888–98. https://doi.org/10.1002/er.2891.
[6] Klonowicz P, Witanowski L, Suchocki T. Selection of optimum degree of partial admission in a laboratory organic vapour microturbine. Energy Convers Manag 2019;202:112189. https://doi.org/10.1016/j.enconman.2019.112189.
[7] Brenkacz L, Zywica G, Bogulicz M. Selection of the oil-free bearing system for a 30 kW ORC microturbine. J Vibroengineering 2019;21(2):318–30. https://doi.org/10.21595/jve.2018.19980.
[8] Kozanecki Z, Lagodzinski J. Magnetic thrust bearing for the ORC high - speed microturbine. Solid State Phenom 2013;198:348–53. https://doi.org/10.4028/www.scientific.net/SSP.198.348.
[9] Kicinski J, Zywica G. Prototype of the domestic CHP ORC energy system. Bull Pol Acad Sci-Tech Sci 2016;64(2):417–24. https://doi.org/10.1515/bpasts-2016-0047.
[10] Fujikawa Y. Trends in externally pressurized gas bearings. J Jpn Soc Tribol 2001; 46(2):135–40.
[11] Schweitzer G. Applications and research topics for active magnetic bearings. IUTAM Symp Emerg Trends Rotor Dyn 2011;25:263–73. https://doi.org/10.1007/978-94-007-0020-8_23.
[12] Yang H, Ru B, Shi J. Development of ceramic sliding bearing. Prog Mach Technol 2004:1007–11.
[13] Zheng D, Gu L, Wang T, Wang L. Performance and failure modes of grease lubricated hybrid ceramic bearing in high speed and high temperature condition. Proc ASME/STLE Int Jt Tribology Conf 2013:259–61.
[14] Mancuzo M, Neto R, Cavallini A, Steffen V. Design and implementation of a low-cost active magnetic bearing. J Vib Eng Technol 2023. https://doi.org/10.1007/s42417-023-01018-z.
[15] Zywica G, Baginski P. Investigation of unconventional bearing systems for microturbines. Adv Mech Mach Sci, Mech Mach Sci 2019;73. https://doi.org/10.1007/978-3-030-20131-9_339.
[16] Colombo F, Lentini L, Raparelli T, Trivella A. The challenges of oil free bearings in micro-turbomachinery. Proc 14SDG Workshop 2021: IFTOMM Sustain Dev Goals 2022;108:403–11. https://doi.org/10.1007/978-3-030-87383-7_44.
[17] Witanowski L, Ziolkowski P, Klonowicz P, Lampart P. A hybrid approach to optimization of radial inflow turbine with principal component analysis. Energy 2023;272:127064. https://doi.org/10.1016/j.energy.2023.127064.
[18] Parkins DW, Horner D. Tilting pad journal bearings–measured and predicted stiffness coefficients. Tribology Trans 1993;36:359–66. https://doi.org/10.1080/10402009308983170.
[19] Synnegard E, Gustavsson R, Aidanpaa JO. Influence of cross-coupling stiffness in tilting pad journal bearings for vertical machines. Int J Mech Sci 2016;111–112: 43–54. https://doi.org/10.1016/j.ijmecsci.2016.03.017.
[20] White MF, Torbergsen E, Lumpkin VA. Rotordynamic analysis of a vertical pump with tilting-pad journal bearings. Wear 1997;207:128–36. https://doi.org/10.1016/S0043-1648(96)07469-8.
[21] Li M, Liu X, Zhu R, Wang X, Bai H, Li F, Li H, Meng G. Rotor dynamics behavior of tilting pad bearing supported turbo-expander considering temperature gradient. J Comput Nonlinear Dyn 2015;11:021004. https://doi.org/10.1115/1.4030831.
[22] Wang W, Li Q, He F, Allaire P. Numerical and experimental stability investigation of a flexible rotor on two different tilting pad bearing configurations. Int J Rotating Mach 2014;2014. https://doi.org/10.1155/2014/697925.
[23] Bang KB, Kim JH, Cho YJ. Comparison of power loss and pad temperature for leading edge groove tilting pad journal bearings and conventional tilting pad journal bearings. Tribol Int 2010;43:1287–93. https://doi.org/10.1016/j.triboint.2009.12.002.
[24] Wang L, Xiong X, Xu H. Dynamic coefficients identification of water-lubricated hybrid bearings used in high-speed spindles with different excitation methods. Shock Vib 2017. https://doi.org/10.1155/2017/2597910.
[25] Peng Y, Chen X, Zhang K, Hou G. Numerical research on water guide bearing of hydro-generator unit using finite volume method. J Hydrodyn 2007;19:635–42. https://doi.org/10.1016/S1001-6058(07)60164-4.
[26] Kim SG, Kim KW. Influence of pad-pivot friction on tilting pad journal bearing. Tribol Int 2008;41:694–703. https://doi.org/10.1016/j.triboint.2007.12.003.
[27] Shin MJ, Hwang JD, Kim C, Cho SY. Analytical techniques of case and pad for 5-pad tilting pad bearing. Adv Mater Res 2012;569:620–3. https://doi.org/10.4028/www.scientific.net/AMR.569.620.
[28] Dmochowski W, Brockwell K. Dynamic testing of the tilting pad journal bearing. Tribol Trans 1995;38:261–8. https://doi.org/10.1080/10402009508983403.
[29] Wu Y, Feng K, Zhang Y, Liu W, Li W. Nonlinear dynamic analysis of a rotor-bearing system with porous tilting pad bearing support. Nonlinear Dyn 2018;94:1391–408. https://doi.org/10.1007/s11071-018-4431-7.
[30] Zhou G, Qiao J, Pu W, Zhong P. Analysis of mixed lubrication performance of water-lubricated rubber tilting pad journal bearing. Tribol Int 2022;169:107423. https://doi.org/10.1016/j.triboint.2021.107423.
[31] Jin Y, Shi Z, Zhang X, Yuan X. Rapid solution for analysis of nonlinear fluid film force and dynamic behavior of a tilting-pad journal bearing-rotor system with turbulent and thermal effects. Friction 2020;8:343–59. https://doi.org/10.1007/s40544-019-0263-9.
[32] Yamada Y, Uesato M, Tanaka M. The tribological performance of PEEK lining bearing. Proc EDF-LMS Workshop, B 2004:1–7.
[33] Zhou J, Blair B, Pitsch D. Experimental performance study of a high speed oil lubricated polymer thrust bearing. Lubricants 2015;3:3–13. https://doi.org/10.3390/lubricants3010003.
[34] Bruce P, Butler JB, Dixon SJ. Like for like performance comparison of PEEK and PTFE thrust bearings for use in vertical pump and motor applications. 18th EDF/Pprime Workshop 2019.
[35] Chatterton S, Gheller E, Vania A, Pennacchi P, Dang PV. Investigation of PEEK lined pads for tilting-pad journal bearings. Machines 2022;10:125. https://doi.org/10.3390/machines10020125.
[36] Zywica G, Kaczmarczyk TZ, Brenkacz L, et al. Investigation of dynamic properties of the microturbine with a maximum rotational speed of 120 krpm - predictions

and experimental tests. J Vibroeng 2020;22(2):298–312. https://doi.org/10.21595/jve.2019.20816.
[37] Schmied J. Application of MADYN 2000 to rotor dynamic problems of industrial machinery. Proceedings of 13th SIRM: The 13th International Conference on Dynamics of Rotating Machinery. Denmark: Copenhagen; 2019. p. 490–500.
[38] Madyn 2000 Documentation, Delta JS AG, December 2020.
[39] Zochowski T., Tribological test for evaluation of natural PEEK [Data set]. Gdańsk University of Technology, doi: 10.34808/b2ee-m576.
[40] Zochowski, T., Tribological test for evaluation of CF30 Black PEEK [Data set]. Gdańsk University of Technology, doi: 10.34808/f6rb-ep27.
[41] Olszewski A, Zywica G, Zochowski T. Design and theoretical analysis of a prototype tilting-pad radial bearing with adjustable clearance. Tribologia 2022;(4):7–16. https://doi.org/10.5604/01.3001.0014.5891.
[42] Chasalevris A, Dohnal F. Improving stability and operation of turbine rotors using adjustable journal bearings. Tribol Int 2016;104:369–82. https://doi.org/10.1016/j.triboint.2016.06.022.
[43] Zhang L, Xu H, Zhang S, Pei S. A radial clearance adjustable bearing reduces the vibration response of the rotor system during acceleration. Tribol Int 2020;144:106112. https://doi.org/10.1016/j.triboint.2019.106112.
[44] European patent EP 3 276 191 A1. Hydrodynamic bearing pad construction. 2018.
[45] National patent (Poland) PL 222617B1. Water-lubricated foil radial plain bearing, in particular for marine propeller shafts, water turbines and water pumps. 2012.
[46] Witanowski Ł, Klonowicz P, Lampart P, Ziółkowski P. Multi-objective optimization of the ORC axial turbine for a waste heat recovery system working in two modes: cogeneration and condensation. Energy 2023;264:126187. https://doi.org/10.1016/j.energy.2022.126187.
[47] Jin Y, Chen F, Xu J, Yuan X. Nonlinear dynamic analysis of low viscosity fluid-lubricated tilting-pad journal bearing for different design parameters. Friction 2020;8:930–44. https://doi.org/10.1007/s40544-019-0310-6.
[48] Ranjan R, Ghosh SK, Kumar M. Fault diagnosis of journal bearing in a hydropower plant using wear debris, vibration and temperature analysis: a case study. Proc Inst Mech Eng Part E J Process Mech Eng 2020;234:235–42. https://doi.org/10.1177/0954408920910290.
[49] Tofighi-Niaki E, Safizadeh MS. Dynamic of a flexible rotor-bearing system supported by worn tilting journal bearings experiencing rub-impact. Lubricants 2023;11. https://doi.org/10.3390/lubricants11050212.